

# MANUFACTURE AND PERFORMANCE OF THE LHC MAIN DIPOLE FINAL PROTOTYPES

M. Modena, K. Artoos, M. Bajko, L. Bottura, M. Buzio, P. Fessia, O. Pagano, D. Perini, F. Savary, W. Scandale, A. Siemko, G. Spigo, E. Todesco, I. Vanenkov, J. Vlogaert, C. Wyss, CERN, Geneva, Switzerland

## Abstract

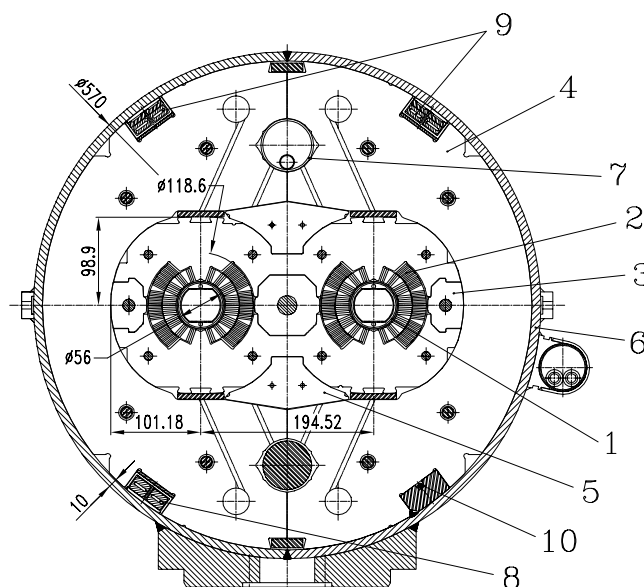
This paper reports about the program of six LHC main dipole final prototypes. This program, launched in summer 1998, relies on industrially manufactured collared coils and cold masses assembled at the CERN Magnet Assembly Facility. The magnet design for series manufacture features a “6-block” coil and austenitic steel collars, following design, stability and robustness studies. Results of mechanical and magnetic measurements are given and discussed, as well as the performances of the prototypes measured so far.

## 1 INTRODUCTION

A program for six final design prototypes was launched in 1998 to validate the design of the LHC main dipoles. Five of the six collared coils produced by the industry are now delivered to CERN. Four cold masses were fully assembled and three of them are already tested. A detailed report about the performance of the first prototype MBP2N1, tested in summer 1999, is given in [1]. In this paper the results of the field quality measurements at room temperature of the prototypes MBP2N2, MBP2O1, MBP2A2 and the power test and field quality measurements at cold of MBP2N1, MBP2N2, MBP2O1 are presented, and briefly analysed.

## 2 MAIN DESIGN FEATURES

The dipole magnet cross-section is shown in Fig.1 and its main parameters are recalled in Table 1. A full description of the salient aspects of the final design adopted can be found in [1]. With respect to the description in [1], the austenitic steel (AS) laminations at both yoke ends have been replaced by an assembly of inner AS laminations and outer low-carbon laminations. This change was introduced to reduce costs by reducing the AS quantity by a factor two whilst maintaining the 15 % field reduction in the coil ends as previously. Further, the quadrupole field component in the ends (a measure of the field asymmetry stemming from the cross-talk between coils) is reduced by a factor three and a full closure of the magnetic circuit is achieved, strongly limiting stray fields in the cold mass ends. This change will be introduced in the last two prototypes.



1-beam tube; 2-SC coils, “6-block” design; 3-austenitic steel collars; 4-iron yoke; 5-iron yoke “insert”, 6-shrinking cylinder / He II vessel; 7-heat exchanger tube; 8-dipole bus-bars; 9-arc quadrupole and “spool-pieces” bus-bars; 10-wires for magnet protection and instrumentation.

Fig. 1. Cross-section of LHC series dipoles:

Table 1: Main parameters of the dipole cold mass.

	Value	Unit
Inject. field (0.45 TeV beam energy)	0.54	T
Nom. field (7 TeV beam energy)	8.33	T
Nominal current	11 800	A
Operating temperature	1.9	K
Magnetic length at 1.9 K	14.300	m
Ultimate operational field	9.00	T
Nominal short sample field limit	9.65	T
Overall length with ancillaries	16.8	m
Mass of the cold mass	~ 30	tonne

## 3 COLLARED COILS

All prototype collared coils, supplied by three European firms, are equipped with instrumented collar-packs based on capacitance load cells [2]. Coil stress measurements have been carried out during all the different assembly

phases and during magnet excitation. Data are presented in Table 2.

Table 2: Coil stresses (in MPa) for inner/outer layers during assembly and test.

Magnet	After collaring (293 K)	After yoking (293 K)	In operation (1.9 K; 0–8.3 T)
MBP2N2	62 / 77	72 / 85	26/32 - 2/8
MBP2O1	51 / 55	62 / 62	24/22 - 0/2
MBP2A2	50 / 52	56 / 60	Not yet tested
MBP2O2	55 / 64	In completion	Not yet tested

## 4 MEASUREMENTS AT ROOM TEMPERATURE, ASSEMBLY

### 4.1 Magnetic Measurements

Warm magnetic measurements at a current of 10 A have been made for four prototypes. Table 3 shows results for “Single-Aperture-Powered” collared coils. The prototypes are shimmed in different ways; N2 has pole-shims slightly thicker than nominal, whilst O1 and A2 feature shims thinner than nominal (up to a few tenths of mm). These differences stem from the fact that the prototypes coils from the three different manufacturers have, for various reasons to be brought under control, slightly different average azimuthal lengths. For each manufacturer, the reproducibility of the coils transverse dimensions is within the specified  $\pm 25 \mu\text{m}$  range, but for the inner layers of O1 ( $\pm 100 \mu\text{m}$ ) because of initial curing moulds problems. The wide variation of  $b_3$  in the three prototypes can be explained by the different pole-shims, using the present sensitivity estimates [3]. For  $b_5$  pole-shim thickness explains part of the variation only, and an unexpected value is found for A2, in both apertures. This is under investigation.

Table 3: Multipole components from the warm measurements for prototype collared coils (Values for the two apertures,  $R_{\text{ref}}=17 \text{ mm}$ ,  $10^4$  units):

	Allowed			Non-allowed				
	$b_3$	$b_5$	$b_7$	$b_2$	$a_2$	$a_3$	$b_4$	$a_4$
N2-1	3.8	-0.2	0.8	-1.2	-2.3	-0.4	-0.4	-0.2
N2-2	2.3	0.0	0.8	1.4	-0.1	-0.2	0.4	0.7
O1-1	-1.1	0.4	0.7	-0.9	-1.1	0.0	-0.1	-0.8
O1-2	-3.0	0.3	0.7	-0.1	1.0	-0.1	-0.1	-0.3
A2-1	-1.9	1.5	0.6	0.3	-2.0	0.2	-0.0	-0.0
A2-2	-1.7	1.1	0.6	-0.7	2.5	0.4	0.2	-0.2

Different shimming approaches were implemented in the prototypes: N2 has the same shims for all coil poles, whilst the other prototypes feature different shim thicknesses (along the coil length in O1 and among apertures in A2) to keep the azimuthal prestress as constant as possible. These differences do not show a

relevant impact on the non-allowed multipoles (see Table 3,  $b_2$  to  $a_4$ ).

The effect of the yoke is rather reproducible: for the analysed cases N2 and O1 we have a shift of around 4 units in  $b_3$  and of 5 units in  $b_2$  (the latter positive for aperture 1 and negative for the other one). The other multipoles are not affected by the yoke by more than 0.1 units). This is in agreement with simulations.

### 4.2 Cold Mass Assembly

The assembly and welding of the cold masses O1 and A2 confirmed the gain in assembly simplicity and time provided by the chosen series-design, as described in [1] for the assembly of the N2 prototype. For the last two prototypes to be assembled, A1 and O2, the first welding pass of the shrinking cylinders will be made by STT welding technology, instead of the MAG one (Ar 96%  $\text{CO}_2$  4%) as previously. The advantages, as confirmed on a 1.5 m long welding model, are a larger, well controllable, weld contraction and the acceptance of larger tolerances for the gap between the shrinking cylinder half-shells. After the first STT pass, five MAG passes, as previously, complete the cylinder welding.

### 4.3 Cold Mass Geometry

The cold mass horizontal curvature, vertical straightness and twist are checked by 3-D measurements carried out with a laser tracker device. Curvature and straightness are within the required tolerance of  $\pm 1 \text{ mm}$ , while for twist the required  $\pm 1 \text{ mrad}$  tolerance is not yet fully achieved. More details can be found in [4].

## 5 TESTS AT 1.9 K

### 5.1 Power tests

Fig.2 shows the initial training for the three cold masses tested up to now. The first prototype is shown for completeness, as it features the series coil design, but an approximated structural geometry, as for scheduling reasons it has aluminium alloy collars from previous work.

Below the ultimate field level of 9 T no quenches occur in the long coil straight sections. This confirms the soundness of the coil cross-section design. All quenches are in the coil ends, mostly in the non-connection one. As observed in the CERN short model programme [5], the behaviour of coil ends depends on pre-stress level, its longitudinal gradient and on manufacturing details. The prototype N2 (where a moderate pre-stress in the coil ends was applied) reaches a higher field level and with less instabilities than N1 (where it had not be possible to apply a well-defined pre-stress to the coil ends). The O1 prototype features light pre-stress in the coil ends and an improved matching between end-spacers and conductor. It trains faster and without instabilities up to 9.15 T, well above the ultimate field.

## 5.2 Field Quality

Cold magnetic measurements have been made on three prototypes. Data for injection field and nominal field are given in Table 4 for N2 and O1 (for N1 see [1]). Because of the two-in-one design, a residual  $b_2$  and  $b_4$  are also among the allowed multipoles

Table 4: Multipole components at injection (0.54 T) and nominal (8.33 T) field. ( $R_{ref}=17$  mm,  $10^4$  units)

Inject.	Allowed					Non-allowed		
	$b_3$	$b_5$	$b_7$	$b_2$	$b_4$	$a_2$	$a_3$	$a_4$
N2-1	-1.1	0.5	0.2	-5.1	0.4	-1.7	0.4	-0.2
N2-2	-2.3	0.6	0.3	4.6	-0.3	-0.0	-0.0	0.4
O1-1	-3.2	0.8	0.3	-4.7	0.2	-1.1	-0.3	-0.7
O1-2	-5.1	0.6	0.2	5.3	-0.1	1.9	-0.2	0.3
Nom.	Allowed					Non-allowed		
N2-1	6.8	-0.6	0.6	-4.7	0.2	-1.6	0.3	-0.1
N2-2	5.8	-0.5	0.6	4.4	-0.2	0.2	0.1	0.5
O1-1	4.6	-0.4	0.6	-4.5	0.1	-0.5	-0.2	-0.6
O1-2	2.8	-0.5	0.6	5.1	0.1	1.4	-0.1	0.3

With respect to the room temperature measurements of the assembled cold mass, at injection one has the main contribution of persistent currents and an additional effect of deformations due to cooling down from 293 K to 1.9 K. This mainly affects  $b_3$  (-7 units),  $b_5$  (+0.5 units) and  $b_2$  (+1 unit). At high field, persistent currents disappear and the effect of iron saturation is present, mainly shifting  $b_3$  (+8 units) and  $b_5$  (-1 units). The contribution of persistent currents and iron saturation is very similar in all the analysed apertures. The effect of cooling down is also very similar for apertures belonging to a same magnet, but features some differences when comparing N2 to O1, especially in  $b_3$  (around 2 units). This value can be explained considering the differences of coil prestress at 293 K and 1.9 K.

The field quality features a spread in  $b_3$  and  $b_5$  mainly due to different shim sizes, as already observed in the collared coil data. A fine-tuning is foreseen for the pre-

series production. The  $b_2$  (5 units in all apertures) will be reduced by an easy minor modification of the insert shape, to be tested in the prototype A2.

## 6 CONCLUSION

The program of six final design prototypes launched in 1998 to validate the design of the LHC main dipoles is approaching its conclusion. Five of the six prototype collared coils were delivered to CERN, four cold masses are fully assembled, three are measured and tested, the two remaining prototypes will be assembled and tested by the end of the year. A first evaluation of the results shows that the nominal field is exceeded after one to three quenches, and quenches below 9 Tesla occur only in the coil ends, a point which is being actively studied in the short model programme [5]. The magnetic field quality analysis is ongoing. The results seem coherent with the mechanical and geometrical characteristics of each prototype. The manufacturing, assembling, measuring and testing details and procedures developed and optimised during the prototype programme, are now being transferred to the pre-series production (for 90 cold masses) launched by CERN in June 1999.

## REFERENCES

- [1] K. Artoos et al, "Design, Manufacturing Status, First Results of the LHC Main Dipole Final Prototypes and Steps Towards Series Manufacture" Presented at the MT-16. IEEE Trans. Appl. S.C., **10** (2000) 98
- [2] N.Siegel, D.Tommasini, I.Vanenkov, "Design and Use of Capacitive Force Transducers for Superconducting Magnet Models for the LHC", MT-15, Beijing, LHC Project Report 173.
- [3] P. Ferracin et al, "Thermo-mechanical Model of the LHC Main Dipole Structure and Assessment of Field Quality", this Conference.
- [4] M. Bajko, F. Savary and W. Scandale, "Geometry and alignment requirements for the LHC main dipole", this Conference.
- [5] D. Tommasini et al., "Status of the LHC short Dipole Model Programme", this Conference.

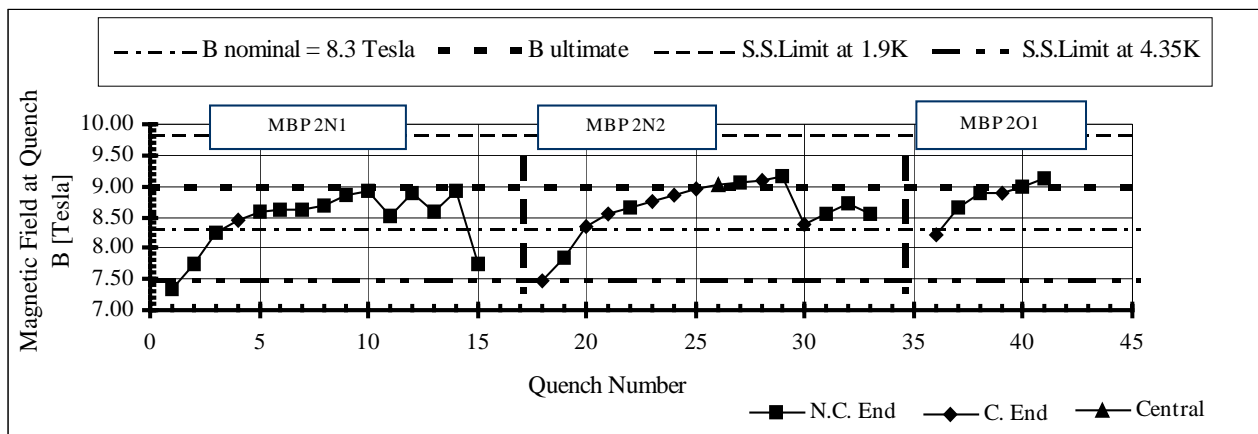


Fig.2. History of the training quenches